JOTCS A
Journal of the Turkish Chemical Society
Section: A
Chemistry

TURKISH
CHEMICAL SOCIETY

Preparation and characterization of Co-doped TiO_2 for efficient photocatalytic degradation of Ibuprofen

Hatice Çağlar Yılmaz*, Ceren İlhan, Emrah Akgeyik, Sema Erdemoğlu

İnönü University, Department of Chemistry, Art and Science Faculty, Malatya, Turkey.

Abstract: Photocatalytic degradation of Ibuprofen (IBU) which is an anti-inflammatory drug was investigated in aqueous solution by Co-doped TiO_2 and bare TiO_2 synthesized by reflux route. The prepared catalyst powders were fully characterized using X-ray diffraction (XRD), FT-IR spectroscopy, scanning electron microscopy (SEM), BET surface areas, X-ray Fluorescence Spectroscopy (XRF), dynamic light scattering (DLS). Efficiency of photocatalytic activity for synthesized Co-doped and bare TiO_2 was evaluated for the degradation of IBU under UV-C and visible irradiation by investigating the effects of cobalt doping percentage, amount of catalyst, irradiation time, initial IBU concentration, pH and also the effect of organic and inorganic matrix. At optimum degradation conditions under UV-C light and visible light, photocatalytic degradation rates were monitored using UV/Vis spectrophotometer, HPLC and Total Organic Carbon (TOC) analysis. The results showed up the degradation of IBU was improved upon Co doping. It was detected that complete removal was achieved within 240 min of irradiation under UV-C and 98% of IBU was decomposed under visible light in 300 min.

Keywords: Co-doped TiO_2, wastewater, veterinary drugs, ibuprofen, advanced oxidation techniques.

Submitted: January 25, 2021**. Accepted:** April 07, 2021**.**

Cite this: Çağlar Yılmaz H, İlhan C, Akgeyik E, Erdemoğlu S. Preparation and characterization of Co-doped TiO2 for efficient photocatalytic degradation of Ibuprofen. JOTCSA. 2021;8(2):553–66.

DOI: https://doi.org/10.18596/jotcsa.855107.

Corresponding author. E-mail: hatice.caglar@inonu.edu.tr

INTRODUCTION

Marine pollution results from several causes, such as wastewater discharge from industrial and commercial sources, products that contain chemical substances, and widespread usage of medical and cosmetic products by human beings (1). Pharmaceutical pollution has attracted particular attention both due to limited information on its effects on the environment and its possible deadly impacts on wildlife, humans, and aquatic ecosystems (2). One of the pharmaceuticals with a wide range of usage is ibuprofen, an NSAID (a non-steroidal anti-inflammatory drug) with low solubility in water (0.021 mg/mL at 20 °C) but is quite soluble in most organic solvents. Its usage areas include the treatment of fever, pain and inflammation, migraines, and rheumatoid arthritis. Ibuprofen's direct and indirect use in everyday life can lead to leaching into groundwater and soil, just like other pharmaceuticals. The elimination of pharmaceuticals is important as drug degradation is not widely included in traditional wastewater treatment facilities (3).

The elimination of resistant toxic chemicals is necessary to degrade pharmaceutical organic pollutants found at different amounts in various water sources and ensure quality drinking water is available. To this end, various methods, including chemical oxidation through chemical-physical and biological processes, are used. Since persistent organic pollutants (POPs), which have toxic impacts on microorganisms, are resistant to known environmental degradation processes, biological processes fail to eliminate such pollutants in

wastewater. For this reason, more effective degradation techniques must be developed (4). The process of chemical oxidation, which is not a cost-effective method for the degradation of pollutants at high concentrations, is not appropriate for eliminating all organic pollutants. For this reason, the removal or degradation of persistent organic pollutants required the development of a number of oxidative degradation processes. Degradation and removal methods are classified into two groups: Photochemical Advanced Oxidation Processes and Ozonation Processes. Many studies conducted in recent years on advanced oxidation techniques aimed to achieve the degradation of persistent organic pollutants by using heterogeneous semiconductor photocatalysts such as ZnO, Fe_2O_3, TiO_2. These studies focused especially on removing textile dyes from wastewater. Free hydroxyl radicals are formed by heterogeneous photocatalysis, particularly the absorption of under 400 nm light. The formed free radicals are later used in the degradation of organic pollutants. With its high photocatalytic activity, superior functionality, and low cost, TiO_2 has an important place in advanced oxidation technology.

Nevertheless, the rapid electron-hole recombination has a decreasing effect on the photocatalytic activity of TiO_2 (5). The introduction of extra components, including metallic and non-metallic doping elements into TiO_2, would reduce the bandgap of TiO_2 and shift the light absorption ability to the visible region (6). Furthermore, because of its large bandgap (3.2 eV), TiO_2 has no activity under visible light. Various methods have been used to make use of sunlight. This can be achieved by doping transitional metal ions such as Ni, Co, Fe, Cu, V, or non-metal doping such as S, N (7,8,9,10). Hence, some of the major concerns for enhancing the photocatalytic activity of TiO_2 include a decrease in the work function for reaction, suitable bandgap to seize visible light, and higher carrier mobility for lower rates of recombination of electrons and holes. Co-doped TiO_2 has drawn particular attention among these metals because cobalt has electrical, catalytic, magnetic, and optical characteristics. Therefore, it is widely utilized in electromagnetic and photocatalysis applications (11). In many studies, advanced oxidation processes (AOP) have been used for the degradation of NSAID. In order to increase these degradation rates, the studies in which H_2O_2 or O_2 (by pumping) is added to the medium where photocatalysts are found (12). However, in this study, although H_2O_2 or O_2 was not added to the medium, quite high photoactivity was achieved with the synthesized Co-TiO_2. Many study in the literature have mostly focused on the use of commercial TiO_2, known as Degussa P25 and Hombikat UV-100, in suspension form. These commercial catalysts have disadvantages such as having low surface area of 40-60 m^2/g, being excited by UV light and only 5% of the sun (13). In the present study, the reflux technique was used to synthesize Co-doped TiO_2 for Ibuprofen's photocatalytic degradation in aqueous solutions under UV-A or UV-C light.

EXPERIMENTAL SECTION

Materials

Titanium isopropoxide ($Ti(OPri)_4$) $C_{12}H_{28}O_4Ti$ (97 wt. %) was provided from Alfa Aesar. 2-propanol (≥99.5 wt.%), ethanol (99 wt.%), cobalt acetate tetrahydrate, methanol (HPLC grade), potassium hydrogen phosphate, tannic acid, gallic acid, and Ibuprofen (IBU) were provided by Sigma Aldrich. Hydrochloric acid (37 wt.%) was purchased from Riedel de Haën. Potassium nitrate, magnesium chloride, sodium phosphate, calcium sulfate, potassium carbonate, sodium hydroxide, and potassium chloride were purchased by Merck.

Catalyst synthesis

Bare and Co-doped TiO_2 nanoparticles (NPs) were synthesis by a reflux method (14). Applied synthesis stages are given in Figure 1. For the preparation of bare TiO_2 NPs, the processes were the same as the method described below in the absence of doping Co^{2+} ion.

Characterization of the catalyst

The NPs were characterized by X-ray diffraction (XRD) pattern recorded using the Rigaku RadB-DMAX II diffractometer. The prepared NPs were determined with Cu Kα (λ = 1.5418 A) radiation at room temperature to characterize the crystalline phase of nanoparticles. Bragg angle is 2θ=25.3° in the region. The crystallite size of nanoparticles was determined from XRD peak of spacing according to the Scherrer's equation given below.

$$D = \frac{K \times \lambda}{\beta ½ \times \cos Q} \qquad \text{(Eq. 1)}$$

The adsorption-desorption isotherms using liquid nitrogen (77 K) were acquired in a Micromeritics Tristar 3030 model equipment to define the specific surface area (S_{BET}) and average pore diameter of all synthesized samples. The NPs specific surface areas and pore size distributions were determined by BET (Brunauer–Emmett–Teller) methodology.

The morphology, size, and size distribution of samples were investigated by Leo Evo 40 Model scanning electron microscopy (SEM) equipped with energy-dispersive X-ray spectroscopy (EDX) was used. Hydrodynamic diameter, zeta potential, and particle size distribution of the NPs were defined by a Malvern Zetasizer Nano-ZS model using the dynamic light scattering (DLS) method. Elemental

analysis and chemical composition of NPs was determined using PANalytical Axios^{MAX} model energy-dispersive X-ray spectroscopy. X-ray Fluorescence Spectroscopy (XRF) was employed to determine the atomic percentage of the Co^{2+} with respect to titanium. The phase purity and monitoring functional groups of NPs were defined by Fourier-Transform Infrared (FT-IR) spectra. The infrared spectra were acquired on an FT-IR spectrometer (Spectrum 1000, Perkin Elmer).

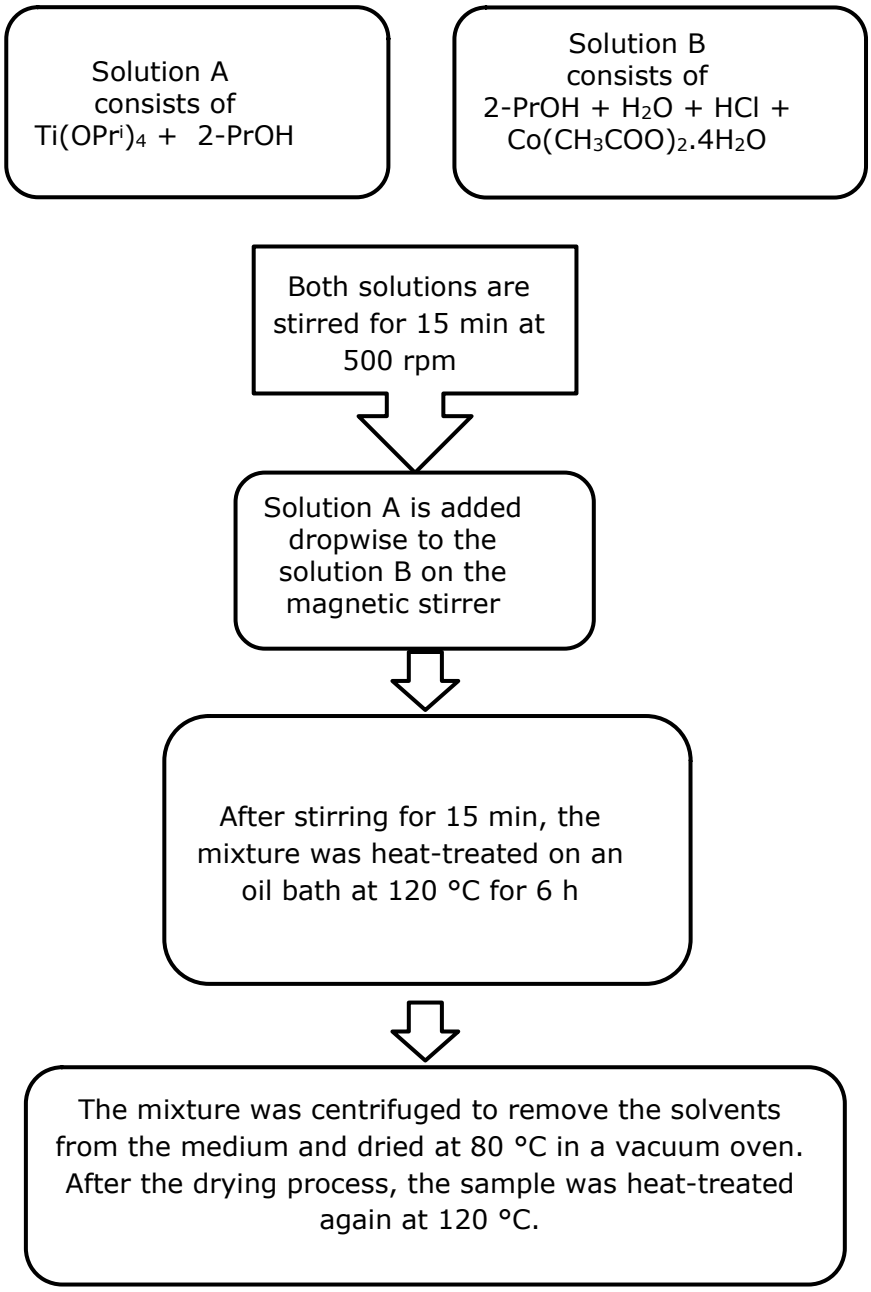

Figure 1: The schema of synthesis of Co-doped TiO_2 NPs.

Evaluation of the photocatalytic performance of IBU

To use in the degradation experiments for IBU, the stock IBU solution was prepared at 100 mg/L in ultrapure water and held in an ultrasonic bath for complete dissolution. Deionized water used in all experimental studies was provided from the Elga Purelab distillation unit. All standard solutions were diluted from the stock solution, and all solutions were stored at -5°C in dark glass bottles for one month. Photocatalytic degradation studies were performed in an Erichsen 1500 model solar box unit

with a Xe lamp (Erichsen, Germany) and controllers for irradiation time and intensity of light. UV light transmission was interrupted with a cut-off filter (yellow filter), and photocatalytic studies were performed under visible light. At first, the predetermined amount of catalyst was added into a dilute solution of IBU in a 50 mL polystyrene transparent beaker placed in the dark to ensure adsorption-desorption equilibrium for 90 minutes at room temperature. According to UV-Vis spectrophotometric measurements, no significant change in the IBU concentration in the solution was observed when the adsorption-desorption equilibrium was reached.

The solution was irradiated immediately. After irradiation, the solution was filtered with a 0.45 µm membrane filter. Degradation of IBU by photolysis without catalysts was also irradiation under UV-C light in the solar box. Change of the IBU concentration in the solution during the degradation process was measured by a UV-Vis spectrophotometer (Varian Cary 50, λmax=224 nm for IBU), and total organic carbon (TOC) in the solution before and after the irradiation was determined using a TOC analyzer (Teledyne Tekmar TOC Torch).

To determine the experimental conditions for degradation of IBU, the influence of the parameters such as the amount of catalyst, percentage of Co-doped TiO_2, pH, irradiation time, and initial concentration of IBU were investigated. The degradation efficiency was calculated using the following equation,

$$Degradation\,efficiency\,(\%)=\frac{(C_t-C_0)}{C_0}\times 100 \quad \text{(Eq. 2)}$$

where C_0 represents the first concentration, C_t is the residual concentration of after irradiation at the time (t). The correlation of ln C_0/C_t with irradiation time (t) was used to determined degradation kinetics.

In order to define the effect of the matrix on the photocatalytic degradation process, various anions and cations, as well as organic substances such as gallic and tannic acid, were added to the irradiation medium. The concentration of IBU before and after the photocatalytic degradation process was determined using an Agilent 1100 series HPLC equipped with a photodiode array detector and Zorbax Eclipse XDB-C_{18} column. The mobile phase consists of 20% MeOH and 80% KH_2PO_4 (pH:3) mixture. Dynamic calibration range was 0.5-30 mg/L, LOD was 0.15 mg/L, and R^2=0.9992 by HPLC-DAD for IBU. Every photocatalytic experiment was done in triplicate.

RESULTS AND DISCUSSION

Characterization of bare and Co-doped TiO_2

Figure 2 shows XRD diffraction patterns for reflux-synthesized bare TiO_2 and Co-doped TiO_2, XRD patterns exhibit strong diffraction peaks at 25.24°, 37.62°, 48.22° and 54.72° 2θ indicating the presence of TiO_2 in the anatase phase, rutile and brookite phases were not detected, no peaks associated with separated cobalt oxide phases such as Co_3O_4 were detected. This could be either explained by the fact that the Co^{2+} ions have been doped into the TiO_2 lattice since the Co^{2+} ions (0.65 Å) are smaller than that of Ti^{4+} (0.69 Å) (15), or due to the low concentration of cobalt ions to be detected.

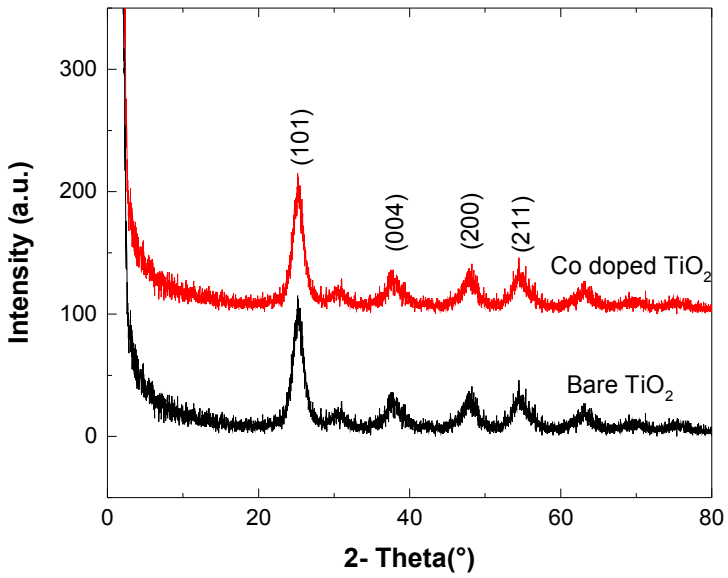

Figure 2: XRD patterns of bare and Co-doped TiO_2 catalysts.

According to the calculations obtained in the Scherrer's equation, the average crystallite size of the bare TiO_2, Co-doped TiO_2 is much lower compared to commercial Degussa P25. It was estimated to be 9.3, 9.2, and 30 nm, respectively. The specific surface area of bare and Co-doped TiO_2 was determined by the Brunauer-Emmett-Teller (BET) method. It was demonstrated that de Co-doped titanium dioxide has a higher specific surface area with 209 m^2/g compared to the bare titanium dioxide and Degussa P25 with 198 and 56 m^2/g, respectively. The synthesized samples' microstructure and external morphology can be explained by the SEM characterization technique presented in Figure 3. The particle shape shows similarities and irregular blocks due to agglomeration. These results were in good agreement with the XRD pattern, which did not show any clear cobalt oxide peaks in the composite.

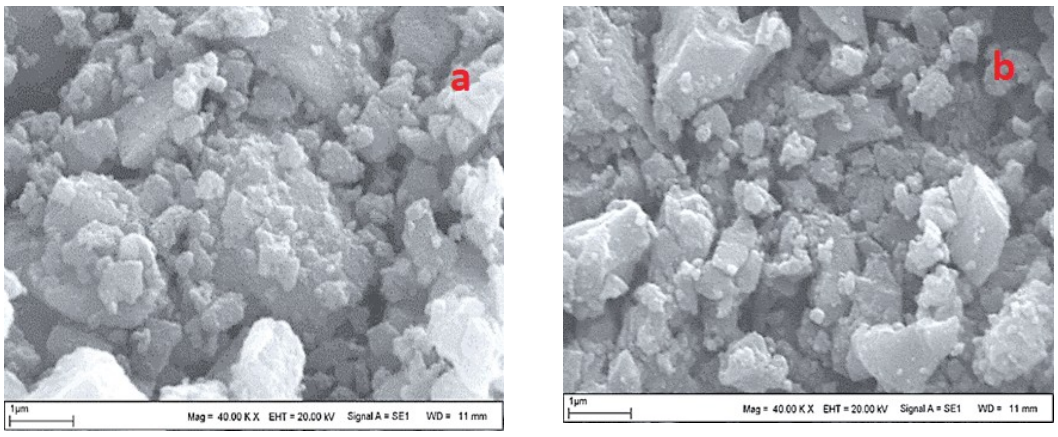

Figure 3: SEM images of bare TiO_2 (a) and Co doped TiO_2 (b).

To confirm the cobalt oxide concentration in the synthesized materials, a full elemental analysis was carried out after the synthesis. EDX results of elemental analysis of Co-doped TiO_2 verified Ti, O, Co, and Cl elements with elements contents of 31.76%, 65.61%, and 0.29% 2.34% (by weight), respectively compared to bare TiO_2 that confirmed the absence of cobalt ions. The chemical composition of TiO_2 samples was identified with X-ray fluorescence (XRF) analysis. The XRF results are summarized in Table 1.

Table 1: Results of XRF of the synthesized bare TiO_2 and Co-doped TiO_2 catalysts.

	Bare TiO_2 (wt. %)	Co-doped TiO_2 (wt. %)
TiO_2	97.42	97.03
Co_3O_4	-	0.2115
Cl	2.37	2.41

The XRF results were compatible with EDX results, which approximately show the same cobalt oxide ingredient into the TiO_2 matrix.

It is also significant the agreement between Cobalt content measured by DLS presented in Figure 4 and XRF for the bare and Co-doped TiO_2 indicating the good dispersion of cobalt into TiO_2 matrix and the similar dimension of agglomerates for Co-doped TiO_2.

Figure 5 exhibits the FT-IR spectra of the bare and Co-doped TiO_2 samples. The broad and strong peaks in the range of 400–1000 cm^{-1} can be ascribed to the Ti–O and Ti–O–Ti bonds in the sample. The peak at 3000–3400 cm^{-1} is attributed to the O-H stretching vibration of Ti-OH and water that corroborate hydroxyl groups' presence in the modified TiO_2 catalysts. The broad absorption peak observed at 1620 cm^{-1} corresponds to water -OH bending and C=C stretching.

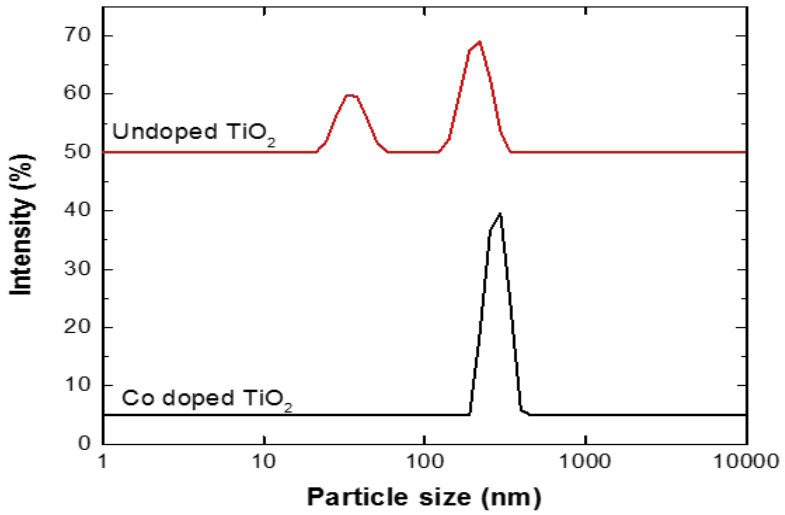

Catalyst	**Size (nm)**
Co doped TiO_2	295
Bare TiO_2	82.8; 255

Figure 4: Particle size distributions of the catalysts according to DLS measurements.

In order to better understand the stability and surface electrostatic charge of the suspended materials, zeta potential values and isoelectric point of bare and Co-doped TiO_2 were determined in aqueous solution at different pH values, using a Zetasizer apparatus. The results are presented in Figure 6 and Table 2. If the systems have a zeta potential higher than ±30 mV in colloidal systems, it is considered stable. As shown in Table 2 and Figure 6, the catalysts' zeta potential is nearly 35 mV up to pH values of 4.

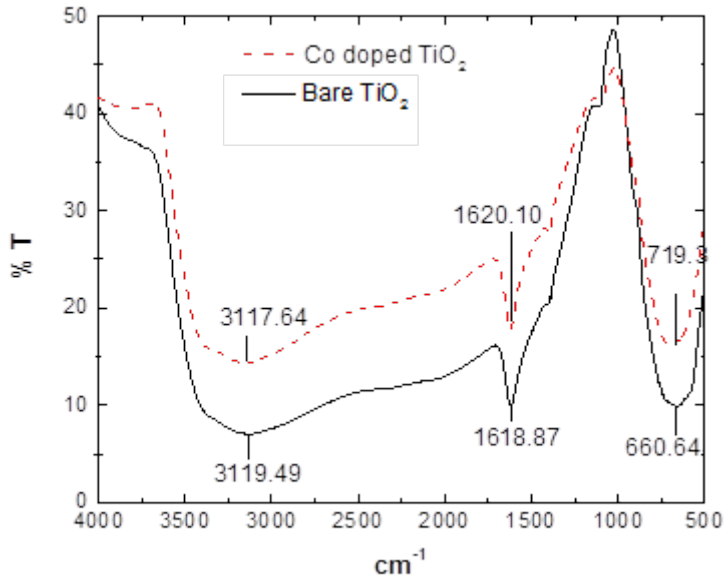

Figure 5: FTIR spectra of bare TiO_2 and Co-doped TiO_2 catalysts.

Table 2: The native pH value, isoelectric point, and zeta potential of bare and Co doped TiO_2.

Catalyst	Zeta potential (mV)	Medium pH	Isoelectric point, pH
Bare TiO_2	35.3 ± 0.3	3.14	6.93
Co doped TiO_2	34.23 ± 1.0	3.07	6.38

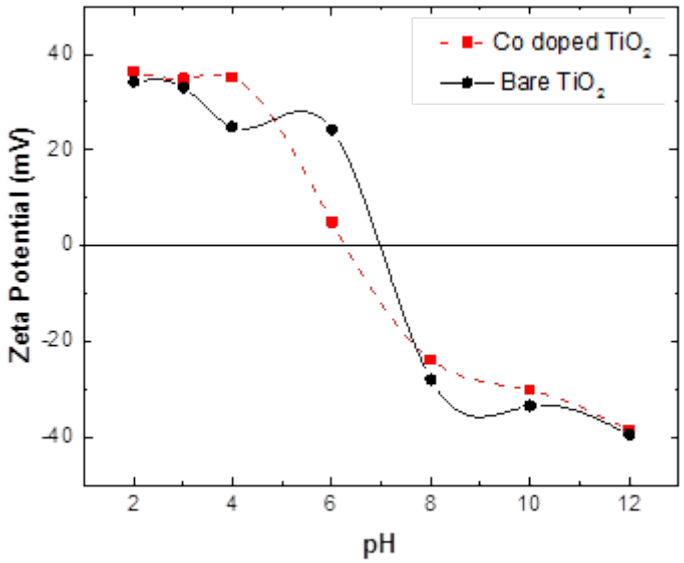

Figure 6: Zeta potentials at different pHs in the 10^{-3} M KCl medium of bare TiO_2.

Effects of parameters on the degradation of IBU

Effect of adsorption and photolysis

Before irradiation, the mixture of catalyst and IBU was soaked in the dark for 90 min at room temperature to reach adsorption equilibrium on the surface catalyst; no significant adsorption effects were observed. The photolysis effect was also investigated and solutions of IBU were irradiated with UV-C radiation at 240 min for the photocatalytic test. After 180 min irradiation under UV-C light, only 2.50% of IBU was degraded.

Effect of cobalt doping percentage

Several tests were performed to observe the effect of cobalt doping percentage on the photodegradation of IBU (Figure 7). The activities were investigated in the range of 0.25–1.0%. It can be observed that the degradation increases with doping concentration from 0.25% (n/n) to achieve

maximum degradation at 0.5% of cobalt doping, but further cobalt concentration increase does not improve degradation, a possible explanation resides in the fact that when the dopants are excessive, cobalt ions may not enter TiO_2 lattice but cover the surface of TiO_2 and form heterogeneity junction so photocatalytic activity is reduced. Furthermore, as the concentration of dopant increases, electron-hole pairs captured overcome the barrier and recombine. On the other hand, 0.5% Co concentration considered as the suitable amount dopant since it can capture photogenerated electrons and decrease the rate of recombination of electron-hole and therefore accelerate the photocatalytic reaction. This result is quite comparable to other reports (16,17) for sprayed Mo/TiO_2 films for similar doping range.

Effect of photocatalyst dosage

The effect of the amount of catalyst on IBU degradation was studied in the range 0.1-0.4 % under pH 4.0, and the results are shown in Figure 8. As seen, IBU degradation increase from 50.33% to 99.7% by increasing catalyst concentration from 0.1 to 0.4%, beyond which the effect is less pronounced. Thus, a solid to liquid ratio of 0.4% could be considered the optimum concentration of catalyst for IBU degradation.

This improvement can be attributed to increasing active sites on the catalyst surface and the light penetration of photo activating light into the solution. Consequently, the formation of electron-hole pairs and reactive hydroxyl radicals on the semiconductor's surface increased, which improved the oxidation of IBU into other intermediates.

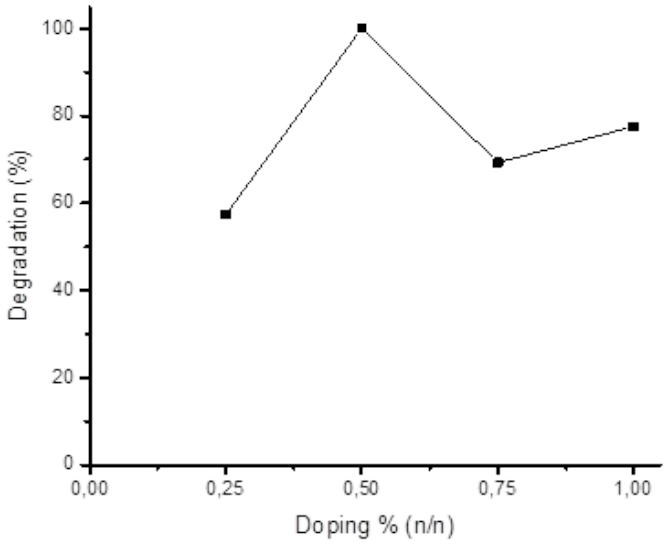

Figure 7: Effect of Co doped on photocatalytic degradation of IBU (20 mg/L, 180 min UV-C irradiation, 670 W/m^2).

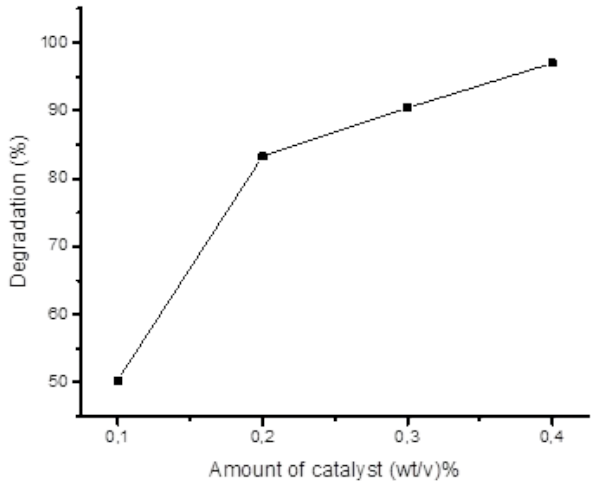

Figure 8: Effect of amount of catalyst on photocatalytic degradation of IBU (20 mg/L IBU, 180 min UV-C irradation, 670 W/m^2).

Effect of irradiation time

The degradation profiles of IBU as a function of irradiation time in the presence of Co-doped TiO_2 is shown in Figure 9. The complete removal of the drug with the initial concentration of 20 mg/L was reached nearly within 240 min of irradiation. It was observed that IBU photodegradation augmented with longer irradiation time directly affects degradation efficiency. After 240 min of irradiation, 99% of IBU was degraded by catalyst under UV light.

In order to determine the kinetics of photodegradation, the correlation between ln C/C_0 and irradiation time was plotted (as inset in Figure 9). As can be seen, a good linear correlation existed between ln C/C_0 and irradiation time, and the degradation reaction obeys the first-order reaction kinetics.

Many authors have reported that the kinetic behavior of photocatalytic reaction can be explained by a modified Langmuir–Hinshelwood model (18). At low concentration, the number of catalytic sites is not a limiting factor, and the rate of degradation is proportional to the substrate concentration, in accordance with apparent first-order kinetics.

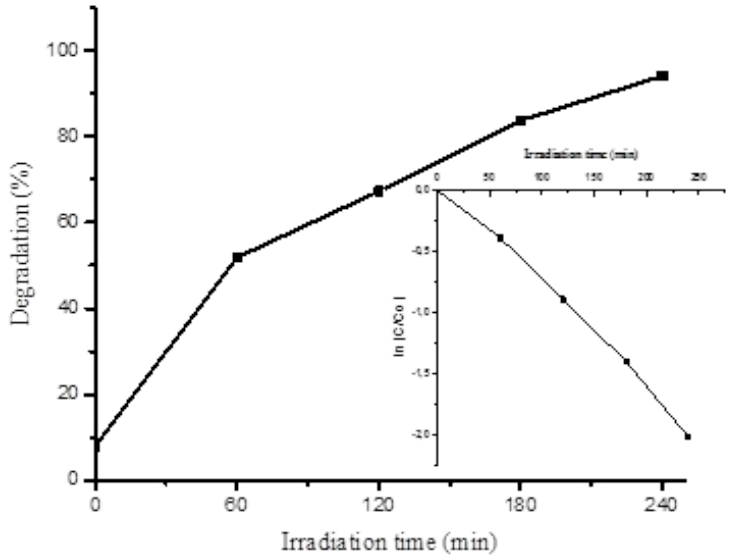

Figure 9: Effect of irradiation time on photocatalytic degradation of IBU (0.4% wt/v catalyst, 20 mg/L IBU, pH: 4.0, UV-C irradiation, 670 W/m^2).

Effect of IBU concentration

The effect of the initial concentration on photocatalytic degradation of IBU was studied for six different concentrations of IBU. For this series of experiments, 0.5% Co-doped TiO_2 was dispersed in 0.4% w/v added into 5, 10, 20, 40, 60, and 80 mg/L IBU solutions, respectively and irradiated under UV-C light during 240 min. Figure 10 illustrates the degradation profile of IBU as a function of the initial concentration. Even at high concentrations of IBU, the photocatalyst activity is high.

Effect of pH

pH is considered an important factor since it affects the surface charge properties of the semiconductor. To study the effect of initial pH on the degradation of IBU with Co doped TiO_2, experiments were conducted by changing the pH in the range 2–10.

As shown in Figure 11, the degradation of IBU strongly depended on the pH solution in the oxidation process. Increased degradation of IBU was observed up to pH 4.0, after which degradation was significantly less effective. When the results are evaluated, the optimum pH for degradation of IBU in an aqueous solution is pH 4. TiO_2 particles tend to form agglomerates when dispersed in alkaline aqueous media. When studied in acidic conditions, agglomeration is reduced, thus increasing the catalyst's effective surface area.

Effect of organic and inorganic water matrix

Wastewater may contain various pollutants; organic solvents and inorganic substances are in general present in industrial water. In order to determine the effect of the organic matrix, gallic acid (170.12 g/mol) as low molecular weight and tannic acid (1701.19 g/mol) as high molecular weight were added as organic compounds commonly found in

real waters. In this study, 0.5% Co-doped TiO_2 was added to 20 mg/L of IBU solution, and the final concentration of the above organic acids was added to the solution as 10, 20, and 30 mg/L; the mixture was maintained over 90 min in the dark to ensure adsorption-desorption equilibrium. Immediately following this, the irradiation experiments were carried out under UV-C light for 240 min. As seen in Figure 12, the presence of organic compounds slightly affects the photocatalytic activity of Co-doped TiO_2 in the degradation of IBU. Thus, the higher the organic compound concentration, the more the deactivation effect, degradation percentage of IBU decreases about 8.11% and 7.25% in the presence of 30 mg/L of tannic acid and gallic acid considered as the large and small molecular weight of organic compounds.

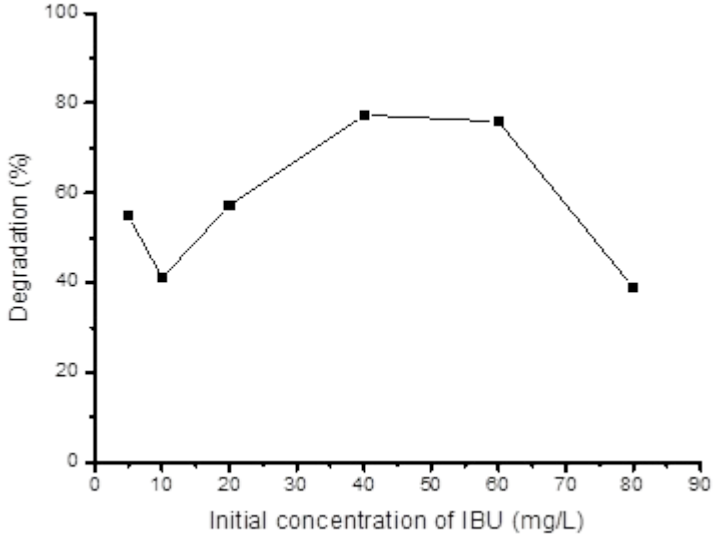

Figure 10: Effect of the initial concentration on photocatalytic degradation of IBU (0.4% wt/v catalyst, pH: 4.0, 240 min UV-C irradiation, 670 W/m^2).

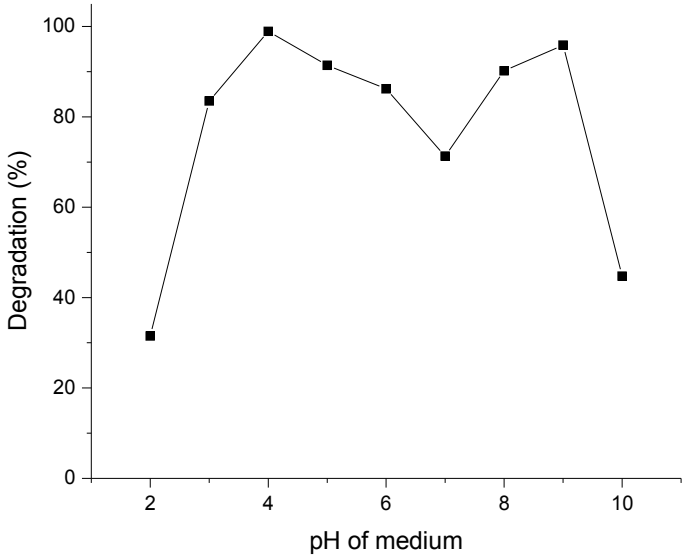

Figure 11: Effect of pH on photocatalytic degradation of IBU (0.4% w/v catalyst, 20 mg/L IBU, 240 min UV-C irradiation, 670 W/m^2).

As can be deduced from Figure 13, the inorganic matrix apparently caused a stronger deactivation effect than the organic matrix. In the presence of inorganic acting as hydroxyl radical scavengers, competition for free radicals and blockage of catalyst active sites by adsorption of anions such as Cl^-, PO_4^{3-}, NO^+, SO_4^{2-}, CO_3^{2-} and cations such as Mg^{2+}, K^+, Ca^{2+}, and Na^+ to form a surrounding layer

that may also be responsible for decreased efficiency of catalyst directly affecting photocatalytic efficiency.

The optimal photocatalytic degradation conditions for IBU are summarized in Table 3.

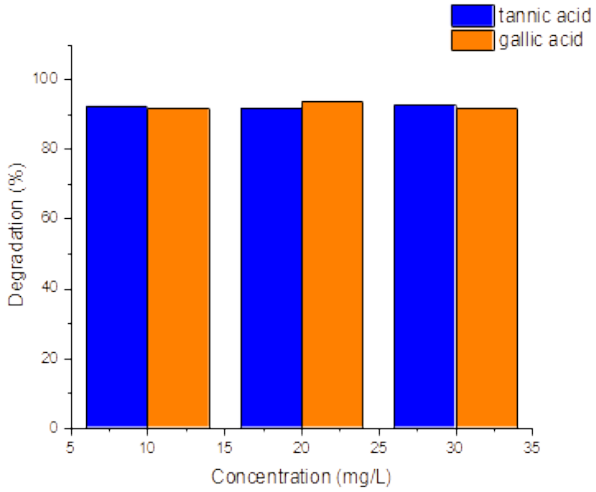

Figure 12: Effect of organic matrix on photocatalytic degradation of IBU (0.4% w/v catalyst, 20 mg/L IBU, 240 min UV-C irradation, 670 W/m^2).

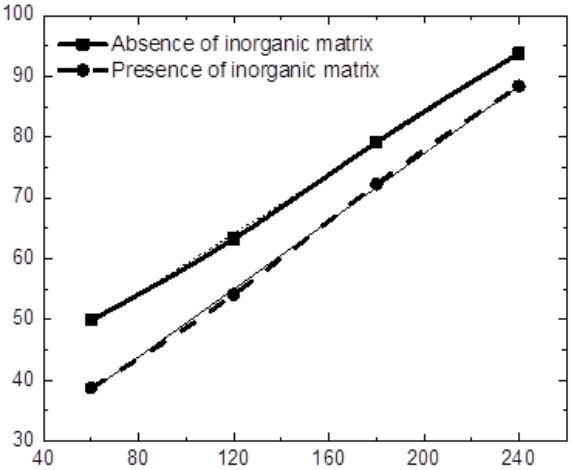

Figure 13: Effect of inorganic matrix on photocatalytic degradation of IBU (0.4% wt/v catalyst, 20 mg/L IBU, 240 min UV-C irradation, 670 W/m^2).

Table 3: The optimum conditions of photocatalytic degradations for IBU.

Conditions	**IBU**
Initial concentration, mg/L	20
Adsorption-desorption equilibrium ,min	90
Amount of catalyst, w/v	0.4
UV light intensity, W/m^2	670
pH	4.0
Illumination time (UV-C), min	240
Illumination time (Vis), min	300

Results of photocatalytic degradation of IBU

The photocatalytic degradation of IBU was studied by liquid chromatographic analysis, UV-Vis analysis, and total organic carbon elimination. The evolution of IBU degradation as a function of time is almost similar for different analytic techniques that confirm the used methods' viability. The maximum degradation rate was obtained at 224 min of

irradiation time with an average degradation rate with different methods of 99.43%.
Maximum IBU absorbance is observed at 224 nm, and with increasing irradiation time from 60 to 240 min, the absorption decreased gradually to a value near blank (Figure 13). The same results were confirmed by HPLC analysis presented in Figure 14 and performed with the same protocol of UV-Vis analysis in order to compare the performance of both analytical methods.

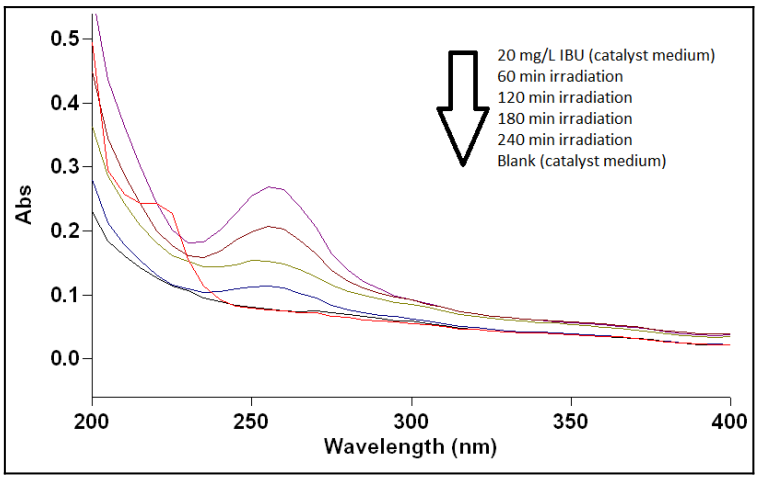

Figure 14: UV-Vis spectrum of the effect of irradiation time on photocatalytic activity of IBU.

The limitation of detection (LOD) and quantification (LOQ) values for IBU degradation are 0.05 and 0.2 mg/L, respectively, according to HPLC analysis and 0.38 and 1.28 mg/L respectively, with the UV-Vis spectrophotometric measurements. The values enable us to evaluate the suitability of the used analytical technique and compare both analytic methods (Table 4).

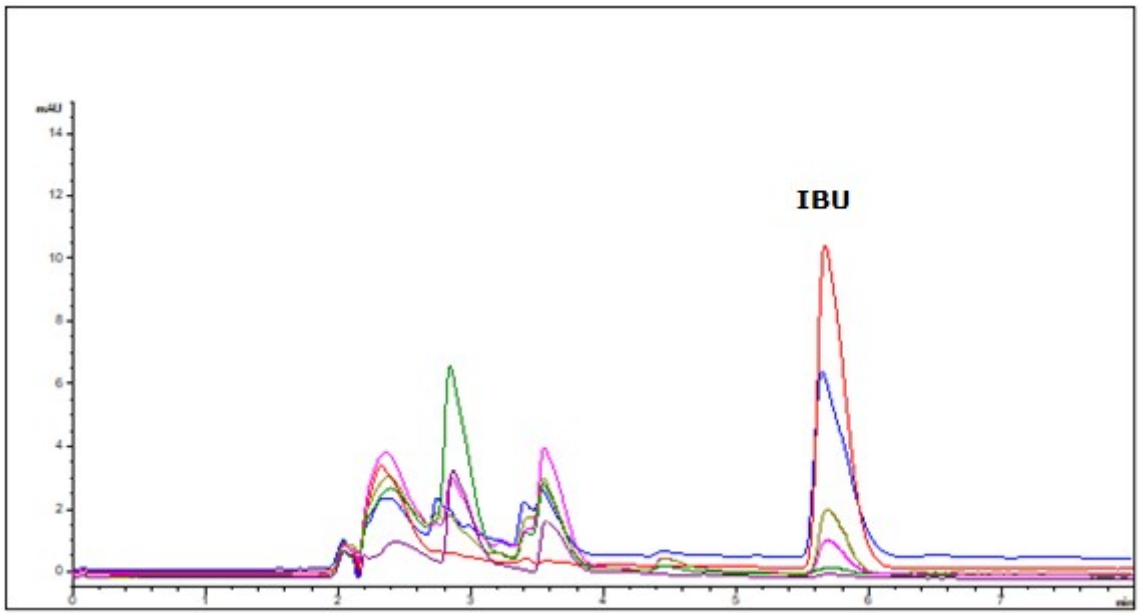

Figure 15. HPLC chromatogram of the effect of UV-C irradiation time on photocatalytic activity (---- 20 ppm IBU (catalyst medium), ----60 min irradiation, ----120 min irradiation, ----180 min irradiation, ----240 min irradiation, ----Blank (catalyst medium).

Table 4: Results of IBU degradation according to different analysis methods.

Catalyst	Degradation ($\bar{x}$ %± sd), n=3					
	UV/Vis Spect. analysis		TOC analysis		HPLC analysis	
	UV-C light, 240 min	Vis light, 300 min	UV-C light, 240 min	Vis light, 300 min	UV-C light, 240 min	Vis light, 300 min
Co-doped TiO_2	100±0.75	98.06±1.12	98.76±2.15	97.04±1.94	99.54±1.14	98.16±2.44
TiO_2	97.56±1.06	24.96±1.99	91.07±2.01	21.97±2.16	93.11±0.99	21.82±1.73
Degussa P25	96.42±2.04	22.25±0.58	90.95±2.26	17.03±2.66	95.47±0.85	19.78±2.13

CONCLUSION

Under UV-C light, the photocatalytic efficiency of Co-doped TiO_2 was found to be as efficient as bare TiO_2 and Degussa P25. Degradation percentage does not present any significant difference between all of them, achieving more than 98% of degradation after 240 min. Under visible illumination, the degradation of IBU shows noteworthy differences with what we observed under UV–C illumination. First, the degradation ratio of bare TiO_2 and Degussa P25 decreases drastically to 24.96% and 22.25% respectively, the low activity of P25 could be explained by the low adsorption of IBU particles on the surface of P25 due to its high pore volume and pore diameter resulting with a decrease in degradation ratio.

The results indicate that the photocatalytic activity of TiO_2 in the visible range is greatly improved by cobalt doping; firstly, Co-doped TiO_2 presents a BET surface area of 209 m^2/g that is fourfold the value of the Degussa P25 (56 m^2/g) and higher than bare TiO_2 198 m^2/g and since the photocatalytic activity increases with increasing BET area which reveals the higher activity. On the other hand, the presence of cobalt can efficiently inhibit the agglomeration of TiO_2 particle, so that Co-doped TiO_2 possesses more active sites than bare TiO_2 and exhibits a higher degradation ratio, it's at least factor 4.5 compared to the other catalyst.

Photodegradation of IBU in aqueous solutions with the catalysis of reflux-synthesized Co-doped TiO_2 with nanocrystalline size (9 nm) was studied. Anatase was the only crystalline phase.

Performance of synthesized bare and Co-doped TiO_2 in photocatalytic degradation under UV-C and visible irradiation was studied by investigating the effects of cobalt doping percentage and catalyst irradiation time, initial IBU concentration pH, and also the effect of inorganic and organic water matrix. The results showed that the degradation of IBU was improved upon Co doping. It was observed that 0.5% Co doping TiO_2 and 0.4% w/v sol could degrade 20 mg/L of IBU within 240 min under UV-C irradiation and 300 min visible irradiation at pH=4.0. The degradation reaction of IBU basically followed the first-order reaction kinetics. Effects of the inorganic and organic matrix on the degradation were examined, and it was found that the inorganic matrix apparently caused a stronger deactivation effect than the organic matrix. Thus, decreases in IBU degradation was observed after 240 min of treatment with 88% of degradation compared to the absence of water matrix with degradation ratio who reaches 93%, whereas organic matrix slightly decreases the degradation ratio.

The results were compared with Degussa P25 TiO_2 at the same degradation conditions; it was found that the synthesized Co-doped TiO_2 showed higher photocatalytic activity than bare TiO_2 and Degussa P25 under visible irradiation.

REFERENCES

1. Gu Y, Yperman J, Carleer R, D'Haen J, Maggen J, Vanderheyden S, et al. Adsorption and photocatalytic removal of Ibuprofen by activated carbon impregnated with TiO_2 by UV–Vis monitoring. Chemosphere. 2019 Feb;217:724–31.

2. Khedr TM, El-Sheikh SM, Ismail AA, Bahnemann DW. Highly efficient solar light-assisted TiO_2 nanocrystalline for photodegradation of ibuprofen drug. Optical Materials. 2019 Feb;88:117–27.

3. Hernando M, Mezcua M, Fernandezalba A, Barcelo D. Environmental risk assessment of pharmaceutical residues in wastewater effluents, surface waters and sediments. Talanta. 2006 Apr 15;69(2):334–42.

4. Sahoo C, Gupta AK. Optimization of photocatalytic degradation of methyl blue using silver ion doped titanium dioxide by combination of experimental design and response surface approach. Journal of Hazardous Materials. 2012 May;215–216:302–10.

5. Park D-W, Choi Y-K, Hwang K-J, Lee J-W, Park JK, Jang HD, et al. Nanocrystalline TiO_2 films treated with acid and base catalysts for dye-sensitized solar cells. Advanced Powder Technology. 2011 Nov;22(6):771–6.

6. Senthilnathan J, Philip L. Photocatalytic degradation of lindane under UV and visible light using N-doped TiO_2. Chemical Engineering Journal. 2010 Jul;161(1–2):83–92.

7. Gar Alalm M, Tawfik A, Ookawara S. Enhancement of photocatalytic activity of TiO_2 by immobilization on activated carbon for degradation of pharmaceuticals. Journal of Environmental Chemical Engineering. 2016 Jun;4(2):1929–37.

8. Hosseini-Zori M. Co-doped TiO_2 nanostructures as a strong antibacterial agent and self-cleaning cover: Synthesis, characterization and investigation of photocatalytic activity under UV irradiation. Journal of Photochemistry and Photobiology B: Biology. 2018 Jan;178:512–20.

9. Siddiqa A, Masih D, Anjum D, Siddiq M. Cobalt and sulfur co-doped nano-size TiO_2 for photodegradation of various dyes and phenol. Journal of Environmental Sciences. 2015 Nov;37:100–9.

10. Sarkar D, Mukherjee S, Chattopadhyay KK. Synthesis, characterization and high natural sunlight photocatalytic performance of cobalt doped TiO_2 nanofibers. Physica E: Low-dimensional Systems and Nanostructures. 2013 May;50:37–43.

11. Hamadanian M, Karimzadeh S, Jabbari V, Villagrán D. Synthesis of cysteine, cobalt and copper-doped TiO_2 nanophotocatalysts with excellent visible-light-induced photocatalytic activity. Materials Science in Semiconductor Processing. 2016 Jan;41:168–76.

12. Lee S-Y, Park S-J. TiO_2 photocatalyst for water treatment applications. Journal of Industrial and Engineering Chemistry. 2013 Nov;19(6):1761–9.

13. Nakashima T, Ohko Y, Tryk DA, Fujishima A. Decomposition of endocrine-disrupting chemicals in water by use of TiO_2 photocatalysts immobilized on polytetrafluoroethylene mesh sheets. Journal of Photochemistry and Photobiology A: Chemistry. 2002 Aug;151(1–3):207–12.

14. Çağlar Yılmaz H, Akgeyik E, Bougarrani S, El Azzouzi M, Erdemoğlu S. Photocatalytic degradation of amoxicillin using Co-doped TiO_2 synthesized by reflux method and monitoring of degradation products by LC–MS/MS. Journal of Dispersion Science and Technology. 2020 Feb 23;41(3):414–25.

15. Colón G, Maicu M, Hidalgo MC, Navío JA. Cu-doped TiO_2 systems with improved photocatalytic activity. Applied Catalysis B: Environmental. 2006 Sep;67(1–2):41–51.

16. Putra EK, Pranowo R, Sunarso J, Indraswati N, Ismadji S. Performance of activated carbon and bentonite for adsorption of amoxicillin from wastewater: Mechanisms, isotherms and kinetics. Water Research. 2009 May;43(9):2419–30.

17. Klauson D, Babkina J, Stepanova K, Krichevskaya M, Preis S. Aqueous photocatalytic oxidation of amoxicillin. Catalysis Today. 2010 Apr;151(1–2):39–45.

18. Li T, Yang S, Huang L, Gu B, Du Y. A novel process from cobalt nanowire to Co_3O_4 nanotube. Nanotechnology. 2004 Sep;15(11):1479–82.